Metal ligand substitution and evidence for quinone formation in taurine/α-ketoglutarate dioxygenase

ARTICLE *in* JOURNAL OF INORGANIC BIOCHEMISTRY · JUNE 2007

Impact Factor: 3.44 · DOI: 10.1016/j.jinorgbio.2007.01.011 · Source: PubMed

4 AUTHORS, INCLUDING:

Tina A Müller
Michigan State University
15 PUBLICATIONS **323** CITATIONS
SEE PROFILE

Melody G Campbell
New York Structural Biology Center
12 PUBLICATIONS **162** CITATIONS
SEE PROFILE

Robert P Hausinger
Michigan State University
179 PUBLICATIONS **9,590** CITATIONS
SEE PROFILE

Available online at www.sciencedirect.com
ScienceDirect
Journal of Inorganic Biochemistry 101 (2007) 797–808
JOURNAL OF Inorganic Biochemistry
www.elsevier.com/locate/jinorgbio

Metal ligand substitution and evidence for quinone formation in taurine/α-ketoglutarate dioxygenase

Piotr K. Grzyska, Tina A. Müller, Melody G. Campbell, Robert P. Hausinger *

Department of Microbiology & Molecular Genetics and Department of Biochemistry & Molecular Biology, Michigan State University, East Lansing, MI 48824-4320, United States

Received 29 November 2006; received in revised form 5 January 2007; accepted 19 January 2007
Available online 3 February 2007

Abstract

The three metal-binding ligands of the archetype Fe^{II}/α-ketoglutarate (αKG)-dependent hydroxylase, taurine/αKG dioxygenase (TauD), were systematically mutated to examine the effects of various ligand substitutions on enzyme activity and metallocenter properties. His99, coplanar with αKG and Fe^{II}, is unalterable in terms of maintaining an active enzyme. Asp101 can be substituted only by a longer carboxylate, with the D101E variant exhibiting 22% the k_{cat} and threefold the K_m of wild-type enzyme. His255, located opposite the O_2-binding site, is less critical for activity and can be substituted by Gln or even the negatively charged Glu (81% and 33% active, respectively). Transient kinetic studies of the three highly active mutant proteins reveal putative Fe^{IV}-oxo intermediates as reported in wild-type enzyme, but with distinct kinetics. Supplementation of the buffer with formate enhances activity of the D101A variant, consistent with partial chemical rescue of the missing metal ligand. Upon binding Fe^{II}, anaerobic samples of wild-type TauD and the three highly active variants generate a weak green chromophore resembling a catecholate–Fe^{III} species. Evidence is presented that the quinone oxidation state of dihydroxyphenylalanine, formed by aberrant self-hydroxylation of a protein side chain of TauD during aerobic bacterial growth, reacts with Fe^{II} to form this species. The spectra associated with Fe^{II}–TauD and Co^{II}–TauD in the presence of αKG and taurine were examined for all variants to gain additional insights into perturbations affecting the metallocenter. These studies present the first systematic mutational analysis of metallocenter ligands in an Fe^{II}/αKG-dependent hydroxylase.

Keywords: Hydroxylase; Non-heme iron; Self-hydroxylation; Spectroscopy; Cobalt

1. Introduction

α-Ketoglutarate (αKG)-dependent dioxygenases are mononuclear non-heme Fe^{II} enzymes that couple the oxidative decarboxylation of an α-ketoacid, usually αKG, to the transformation of a primary substrate [1]. These metalloproteins catalyze a broad spectrum of oxidative reactions including hydroxylations, desaturations, cyclizations, epoxidations, and, as recently demonstrated [2,3], halogenations. The best-characterized representative of this enzyme family is taurine/αKG dioxygenase (also termed taurine hydroxylase or TauD), an *Escherichia coli* enzyme that couples αKG decarboxylation to the hydroxylation of taurine (2-aminoethane sulfonate) as illustrated in Scheme 1 [4].

A reasonable mechanism for Fe^{II}/αKG-dependent hydroxylases, first proposed about 25 years ago [5], is illustrated in Scheme 2. The starting enzyme (A) contains Fe^{II} bound to a two-His/one-carboxylate (Asp or Glu) motif [6,7] with three water molecules completing the six-coordinate environment. Two waters are displaced upon binding of the α-ketoacid, with the cosubstrate chelating the Fe^{II} center through its C-1 carboxylate and C-2 carbonyl moieties (B). The primary substrate binds near the active site and promotes dissociation of the remaining water ligand, thus creating an oxygen-binding site on the five-coordinate

* Corresponding author. Tel.: +1 517 355 6463x1610; fax: +1 517 353 8957.
E-mail address: hausinge@msu.edu (R.P. Hausinger).

0162-0134/$ - see front matter © 2007 Elsevier Inc. All rights reserved.
doi:10.1016/j.jinorgbio.2007.01.011

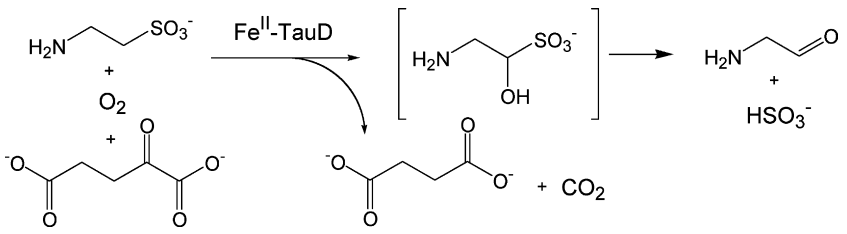

Scheme 1.

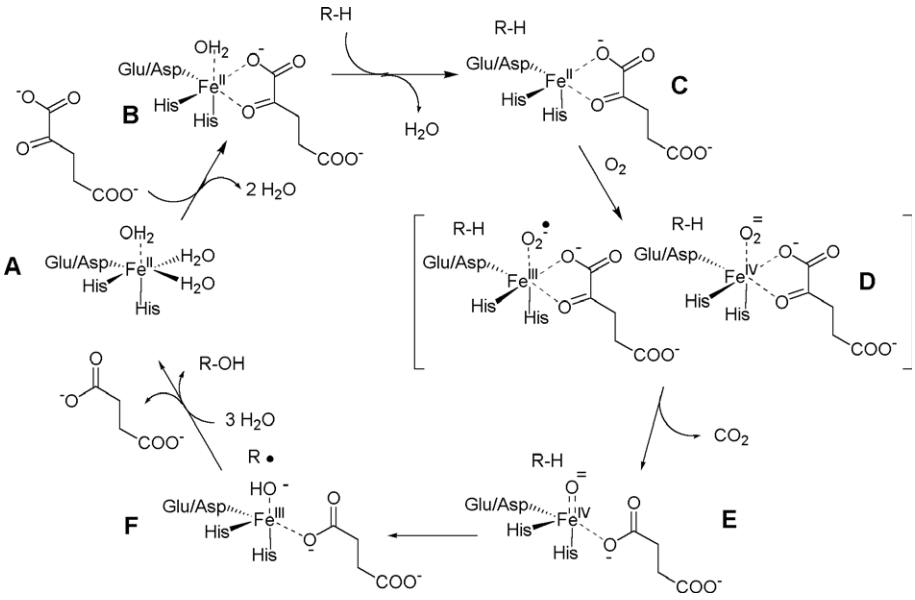

Scheme 2.

Fe^{II} (C). Oxygen addition results in the formation of an Fe^{III}-superoxo or Fe^{IV}-peroxo species (D) that attacks the αKG carbonyl group, leading to αKG decomposition, heterolytic O–O bond cleavage, and production of an Fe^{IV}-oxo species (E). This crucial intermediate abstracts a hydrogen atom from the substrate to form an Fe^{III}–OH intermediate (F) followed by hydroxyl radical rebound to generate product, which dissociates to restore the Fe^{II} state of the enzyme (A).

An extensive series of structural and spectroscopic investigations provide support for several intermediates of Scheme 2. For example, crystal structures of several family members (reviewed in [1,8]) depict the two-His/one-carboxylate ligand architecture that comprises the metal-binding site. In some structures, including that of TauD [9,10], the binding modes of αKG and the primary substrate are revealed. A diagnostic metal-to-ligand charge-transfer (MLCT) transition is associated with the αKG–Fe^{II} complex of the examined enzymes; e.g., TauD exhibits a λ_{max} of 530 nm with ε_{530} 140–240 $M^{-1}\,cm^{-1}$ [11,12]. Binding of the primary substrate perturbs this electronic spectrum, yielding λ_{max} of 520 nm with $\varepsilon_{520} \geqslant 180\ M^{-1}\,cm^{-1}$ for TauD [11], which is attributed to a switch from six-coordinate to five-coordinate metal geometry. Additional evidence for this change in coordination number is available from magnetic circular dichroism studies of clavaminate synthase (CAS) [13–15] and resonance Raman analyses of TauD [16]. Finally, several lines of evidence using transient kinetic approaches support the intermediacy of an Fe^{IV}-oxo species. In particular, the results of stopped-flow ultraviolet (UV)/visible [11,12,17–19], freeze-quench Mössbauer [17], X-ray absorption [20], and continuous-flow resonance Raman [21] investigations combine to convincingly identify this intermediate in TauD. An Fe^{IV}-oxo intermediate also has been identified in a prolyl 4-hydroxylase [22].

To better understand how the metal-binding residues in the 2-His/1-carboxylate motif contribute to the metallocenter properties and enzyme activity, we have carried out a systematic mutational analysis of the archetype Fe^{II}/αKG-dependent hydroxylase, TauD. Although metal ligands have been identified in many αKG-dependent enzymes, the biochemical properties and metal center flexibilities have not been sufficiently explored. Here, the His99, Asp101, and His255 metal-binding ligands of TauD (Fig. 1) were substituted by Ala, incapable of binding metal ions, as well as Asn, Asp (for the two His residues), Cys, Glu, Gln, and His (for the Asp residue). The variant proteins were examined for steady-state activities, transient kinetic properties, Fe^{II} binding, and generation of diagnostic substrate-bound Fe^{II}- and Co^{II}-dependent chromophores, with our

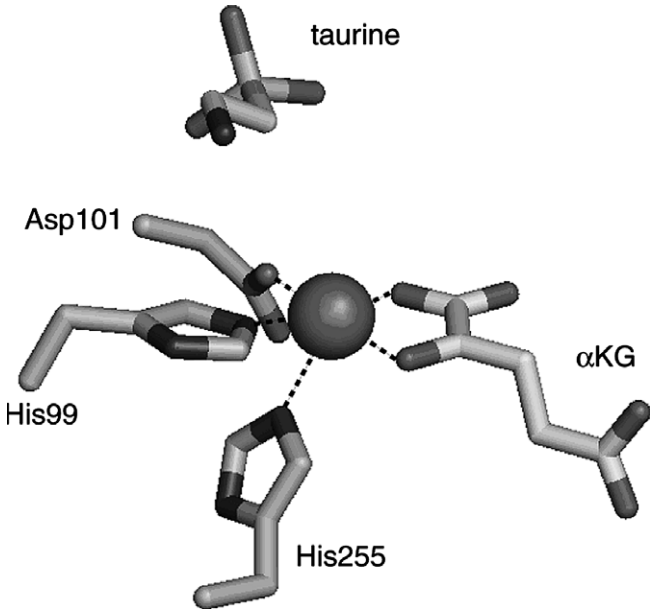

Fig. 1. Enzymatic core of TauD depicting Fe^{II}, its ligands (His99, Asp101, His255, and αKG), and the substrate taurine.

hypothesis being that these properties would be tightly correlated. The addition of formate to the D101A variant led to enhancement of activity, consistent with partial chemical rescue of the missing ligand. In addition, we provide evidence that a covalently bound quinone is responsible for a green chromophore generated by addition of Fe^{II} to anaerobic apoproteins of the active enzymes. These studies present the first comprehensive analysis of metal ligand substitution in any Fe^{II}/αKG-dependent hydroxylase.

2. Experimental

2.1. Enzyme purification and assays

Wild-type TauD and its variants were purified as apoproteins, as previously described [11,23]. Sodium dodecyl sulfate–polyacrylamide gel electrophoresis (SDS–PAGE) [24] was used to monitor fractions containing the inactive variants. Protein concentrations were determined by use of a dye-binding assay [25]. TauD activity was measured by using Ellman's reagent to quantify sulfite, as previously reported [4]. One unit (U) of enzyme activity is defined as the amount of enzyme that releases 1 μmol of sulfite per minute at 30 °C in assay buffer containing 25 mM Tris (pH 8.0), 50 μM Fe^{II}, 100 μM ascorbate, 500 μM αKG, and 1 mM taurine. In selected cases, the buffer was amended with various concentrations of formate or imidazole. For steady-state kinetic analyses, enzyme assays were carried out with varied concentrations of taurine or αKG and collecting single time point data (5–20 min, depending on the activity of the variant). In addition, using 0.64 mM taurine and time points varying from 10 s to 5 min, sulfite production progress curves were generated and analyzed by fitting to Eq. (1), where P_t is the accumulated product at time t, v_i is the initial rate, and k_{inact} is the inactivation rate constant.

$$P_t = v_i \times (1 - \exp(-k_{inact} \times t)) \times k_{inact}^{-1} \quad (1)$$

2.2. Site-directed mutagenesis

The H99A, H99C, H99D, H99E, H99N, H99Q, D101A, D101C, D101E, D101H, D101N, D101Q, H255A, H255C, H255D, H255E, H255N, and H255Q variants of TauD were created by mutagenesis of *tauD* in pME4141 [4] using the Stratagene Quickchange System (Stratagene, La Jolla, CA) as previously described [23], with the plasmids transformed into *E. coli* DH5α (Invitrogen, Carlsbad, CA) and, after sequencing (Davis Sequencing, Davis, CA), into *E. coli* C41 (DE3) [26].

2.3. Fe^{II} binding assay

Aliquots of wild-type or variant TauD samples were diluted into 50 mM imidazole buffer, pH 7.0, at concentrations of approximately 100 μM. Fe^{II} and ascorbate were added from an anaerobic stock solution (containing 25 mM metal ion and 50 mM reductant) to achieve a concentration where Fe^{II} was fivefold over that of the TauD subunit. The samples were incubated for 5 min and rapidly (~1 min) desalted by using a Sephadex G-25 mini-spin column (GE Healthcare). The protein concentrations were reassessed and the Fe contents determined as described by Beinert [27]. Briefly, a sample (100 μL) of each TauD variant with bound Fe^{II} was added to 900 μL of deionized H_2O in a glass test tube, treated with 500 μL of a solution consisting of equal volumes of 4.5% w/v $KMnO_4$ and 1.2 N HCl, incubated at 65 °C for 2.5 h, and mixed with 100 μL of the iron-chelating reagent (containing 9.7 g of ammonium acetate, 8.8 g of ascorbic acid, 80 mg neocuproine, and 80 mg of ferrozine in 25 ml of deionized water). After 30 min at room temperature, the absorbance was measured at 562 nm.

2.4. Spectroscopy

Anaerobic samples of Fe^{II}–TauD, αKG–Fe^{II}–TauD, and taurine–αKG–Fe^{II}–TauD were prepared by subjecting 500 μM TauD subunit (diluted into 25 mM Tris buffer, pH 8.0) to repeated cycles of vacuum and argon purging in an anaerobic cuvette and sequentially amending with 500 μM Fe^{II}, 2 mM αKG, and 2 mM taurine. UV–Vis difference spectra were obtained for the three forms of wild-type and variant enzymes (with the TauD apoprotein spectrum subtracted) as previously described [11]. For selected variants, lower concentrations of TauD subunit were used to minimize precipitation.

To define the basis behind a light green chromophore formed upon addition of Fe^{II} to selected anaerobic TauD samples, the spectroscopy was repeated by using wild-type TauD prepared from anaerobically grown cells and by

using the standard TauD from aerobically grown cells after 30 min treatment with four equivalents of $NaBH_4$. Difference UV–Vis spectra were recorded as above for these samples after addition of 500 μM Fe^{II}, 2 mM αKG, and then 2 mM taurine.

In a manner similar to that for Fe^{II}, the chromophores associated with the binding of Co^{II} to TauD [28] and its variants were examined. In addition, the effects on the Co^{II}-derived chromophores were examined by using 3-*N*-morpholinopropanesulfonic acid (MOPS) and pentanesulfonic acid (PSA), the alternate substrates for the Fe^{II} form of the enzyme. All spectra were corrected to account for sample dilutions.

Stopped-flow UV–Vis spectra were obtained at 4 °C by using a Hi-Tech Scientific model SF-61DX stopped-flow spectrophotometer (1.0 cm path length) in single mixing mode. Oxygen was removed from the instrument by flushing the flow system with anaerobic buffer containing 0.1 U mL^{-1} of protocatechuic acid dioxygenase and 400 μM protocatechuic acid at pH ~7. Anaerobic solutions of TauD and its variants were prepared in a glass tonometer and deoxygenated by repeated cycles of evacuation and purging with argon gas. One syringe was filled with taurine–αKG–Fe^{II}–TauD (500 μM taurine, 500 μM αKG, 500 μM Fe^{II}, and 500 μM wild-type or mutant TauD in 25 mM Tris buffer, pH 8.0) and the other with buffer that had been saturated with 100% oxygen (1.2 mM at 25 °C) or 21% oxygen (air) at room temperature. Kinetic traces were analyzed with KinetAsyst 3 (Hi-Tech) and the data were simulated by using Program A (developed by Chung-Yen Chiu, Rong Chang, Joel Dinverno, and David P. Ballou, University of Michigan, and based on the Marquardt–Levenberg nonlinear fit algorithm [29]), as previously described [12].

2.5. Nitroblue tetrazolium (NBT) quinone staining

TauD and its variants were examined for the presence of a covalently associated redox component by subjecting the proteins (11.5 μg of each) to SDS–PAGE, transferring the proteins to nitrocellulose at 90 V for 90 min at 4 °C in pH 8.3 buffer containing 25 mM Tris, 192 mM glycine, 20% methanol and 0.05% SDS, and using a nitroblue tetrazolium staining procedure that detects quinoproteins [30]. Pre-stained low-range molecular marker proteins (Bio-Rad) were used to confirm the protein size.

3. Results and discussion

Mutagenesis approaches were used to change each of the three TauD metal-binding ligands to Ala, a side chain incapable of serving as a metal ligand, and to five alternative side chain residues that are potential metal ligands. All of the variant TauD samples behave like the wild-type enzyme during purification, consistent with proper folding of the proteins. Two samples, D101H and H255C, are unstable at high concentrations and precipitation problems are exacerbated by the addition of metal ions so they could not be studied in detail. The other metal–ligand variants were extensively analyzed by steady state and transient kinetic studies, metal binding analyses, and anaerobic electronic spectroscopy in the presence of Fe^{II} or Co^{II} and the enzyme substrates.

3.1. Steady state and transient kinetic properties of ligand-substituted TauD variants

The 18 TauD metal–ligand mutants were characterized for their enzymatic activities and compared to that of the wild-type enzyme. As summarized in Table 1, only three variants (D101E, H255E, and H255Q) are sufficiently active to determine their steady-state kinetic parameters. The K_m for taurine and αKG are only modestly affected in these variants. The k_{cat} of the H255E and D101E mutant proteins exhibits 1/3 and 1/5 of the wild-type activity, respectively, whereas that of the H255Q variant approaches that of wild-type enzyme. For the H255E variant, the substantial activity and minor perturbations in the taurine and αKG K_m values were surprising because an additional negative charge is introduced into the active site; in the absence of structural analysis we are unable to offer an explanation for this result. Trace activities also were detected in several other variants, including the cases with Ala replacing the side chains of wild-type enzyme.

Transient kinetic methods previously utilized with the wild-type enzyme [12] were used to qualitatively examine the effects of metal–ligand substitutions on the individual steps of enzyme catalysis in the three active TauD variants. The anaerobic taurine–αKG–Fe^{II}–TauD samples were mixed with buffers saturated with 100% or 21% oxygen while monitoring the changes at 320 nm by using stopped-flow spectroscopic methods (Fig. 2). Each variant protein exhibits a transient increase in 320 nm absorbance, similar to that seen in wild-type enzyme which is known to generate an Fe^{IV}-oxo intermediate that exhibits maximal absorbance near this wavelength [17,21]. The apparent first-order rate constants associated with the formation (k_1) and decay (k_2) of these species (at final O_2 concentrations of 0.121 and 0.575 mM) are shown in Table 2. In each case, the observed k_1 for the formation of the putative Fe^{IV}-oxo species is dependent on the oxygen concentration (i.e., k_1 relates to the rate constant for the reaction of the ternary complex with O_2), whereas k_2 is independent of oxygen concentration. The k_1 and k_2 of the H255E and H255Q variants closely resemble values of wild-type enzyme. Thus, replacement of the imidazole ligand by the equivalent length carboxylate or amide side chains has little apparent effect on the chemical rates associated with Fe^{IV}-oxo formation or its subsequent reaction with substrate. In contrast, the apparent first-order rate constants of formation and decay (with admittedly large error) are significantly smaller for the intermediate in the D101E variant than for wild-type sample, resulting in minimal accumulation of the intermediate. This result is consistent with the

Table 1
Steady-state kinetics and Fe^{II}-binding properties of TauD variants[a]

TauD variant	k_{cat} (s^{-1})	Taurine K_m (μM)	k_{cat}/K_m ($\mu M^{-1} s^{-1}$)	αKG K_m (μM)	k_{inact} (s^{-1})	Fe content (mole Fe/mole subunit)
Wild type	3.30 ± 0.20	19 ± 2.7	0.174 ± 0.035	32 ± 0.8	0.0016 ± 0.0005	0.96 ± 0.12
H99A	0.006 ± 0.001	–	–	–	–	0.75 ± 0.35
H99C	0.009 ± 0.002	–	–	–	–	0.68 ± 0.07[b]
H99D	ND[c]	–	–	–	–	0.93 ± 0.64[b]
H99E	0.021 ± 0.006	–	–	–	–	0.29 ± 0.15[b]
H99N	$\leqslant 0.001$	–	–	–	–	0.19 ± 0.33
H99Q	0.012 ± 0.003	–	–	–	–	0.25 ± 0.28
D101A	$\leqslant 0.001$	–	–	–	–	0.50 ± 0.49[b]
D101C	$\leqslant 0.001$	–	–	–	–	0.78 ± 0.04
D101E	0.74 ± 0.01	61.1 ± 4.5	0.012 ± 0.001	81 ± 5.4	0.0012 ± 0.0003	0.73 ± 0.08
D101H	ND[c]	–	–	–	–	N/A[d]
D101N	$\leqslant 0.001$	–	–	–	–	0.32 ± 0.22
D101Q	0.038 ± 0.001	–	–	–	–	0.16 ± 0.36
H255A	0.003 ± 0.001	–	–	–	–	0.60 ± 0.15
H255C	ND[c]	–	–	–	–	N/A[d]
H255D	ND[c]	–	–	–	–	0.58 ± 0.03
H255E	1.09 ± 0.11	18.9 ± 1.8	0.058 ± 0.011	55 ± 2.6	0.0025 ± 0.0002	0.69 ± 0.38
H255N	0.026 ± 0.005	–	–	–	–	0.58 ± 0.04[b]
H255Q	2.67 ± 0.05	21.9 ± 1.8	0.122 ± 0.012	59 ± 5.1	0.0030 ± 0.0009	0.92 ± 0.19

[a] Data were generated by using Tris buffer at pH 8.0 for the activity assays and imidazole buffer at pH 7.0 for the metal-binding assays. The kinetic studies utilized single-time-point assays except for the k_{inact} studies that used 640 μM taurine. The data shown are not corrected for Fe content.
[b] Some protein precipitation was observed when the protein was incubated with Fe^{II}.
[c] ND, no detectable activity.
[d] N/A, could not examine Fe^{II} binding due to massive protein precipitation.

longer side chain of the carboxylate leading to a shift in position or geometry of the metallocenter so that one or more steps leading to the Fe^{IV}-oxo intermediate is slowed and the rate of reaction with substrate is reduced.

3.2. Activation of the D101A variant by formate

We examined whether additives would affect the activity of variants with a ligand residue replaced by Ala. Supplementation of the assay buffer with formate leads to over fourfold enhancement of the trace level of activity in D101A TauD (Fig. 3), with the k_{cat} increasing from $0.00015 \pm 0.00003\ s^{-1}$ without additive to $0.00087 \pm 0.00013\ s^{-1}$ at 100 mM formate, compatible with partial chemical rescue of the missing ligand by the buffer additive. Half maximal activation was observed at a concentration of approximately 30 mM formate. In contrast, the addition of varied concentrations of imidazole to the standard Tris assay buffer does not significantly increase the activities of the H99A or H255A variants. Indeed, high concentrations of imidazole (greater than 50 mM) lead to reductions in activity of these mutant proteins (data not shown).

3.3. Analysis of Fe^{II} binding by TauD metal–ligand variants

To investigate whether the activities of the TauD variants relate to their capacity to bind Fe^{II}, a simple protocol involving a colorimetric metal assay was used to compare the Fe^{II} binding properties of the proteins. Since we observed large variations in replicate samples and because some metal ions might dissociate during the one-min spin-column procedure, this assay should be considered a qualitative, rather than quantitative, measure of Fe^{II} binding. As shown in Table 1, wild-type TauD retains near stoichiometric amounts of metal ion after this procedure. Similarly, the H99A, H99C, H99D, D101C, D101E, H255A, H255D, H255E, H255N, and H255Q variant proteins also bind more than 0.5 mol of iron per mole of subunit, with small amounts of protein precipitation noted in the H99C, H99D, D101A, and H255N samples. Clear deficiencies in Fe^{II} binding are observed in the H99E, H99N, H99Q, D101N, and D101Q proteins, with some tendency toward precipitation in the H99E sample. Extensive precipitation of the D101H and H255C variants occurs during incubation with Fe^{II}, so their metal contents could not be assessed.

3.4. Fe^{II}–TauD spectra and evidence for a covalently attached quinone in highly active TauD samples

Anaerobic addition of Fe^{II} to TauD samples resulted in the surprising development of a weak and broad absorption near 650 nm in the wild-type enzyme and the D101E, H255E, and H255Q active variants, but this feature was absent in the other samples (see the light dashed lines of Fig. 4 and Fig. S1). Significantly, the intensity of this absorption was found to vary for different preparations of each sample ($\varepsilon_{650} = 86$, 45, 54, and 53 $M^{-1} cm^{-1}$, respectively, for the samples shown). The ~650 nm chromophores generated in these anaerobic samples are much weaker in intensity than, but resemble a mixture of, two previously described spectra associated with catecholate–Fe^{III}

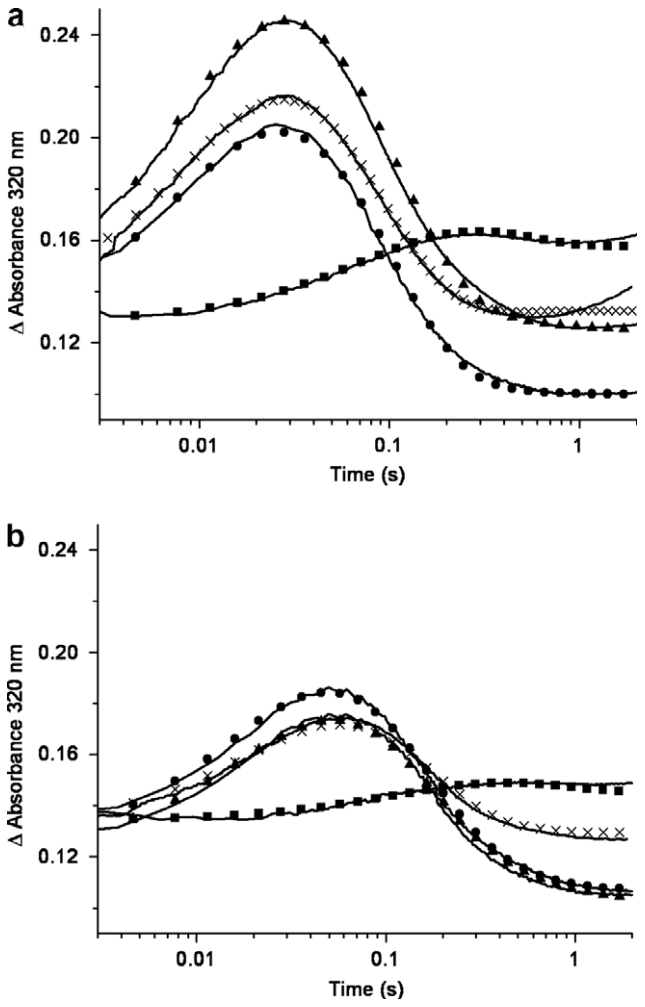

Fig. 2. Stopped-flow UV–Vis kinetics of the Fe^{IV}-oxo intermediate in TauD metal-binding ligand variants. Experimental data are shown by solid lines and the simulations are depicted by the indicated symbols. Anaerobic solutions of the wild-type protein (x) or the D101E (■), H255E (●), and H255Q (▲) variants of TauD (0.5 mM subunit) containing Fe^{II}, αKG, and taurine (0.5 mM, 0.5 mM, and 0.5 mM, respectively) in 25 mM Tris buffer (pH 8.0, 4 °C) were mixed at 4 °C with equal volumes of buffer equilibrated with 100% (a) or 21% (b) O_2 while being monitored in a 1 cm path length flow cell at 320 nm. The apparent first-order rate constants associated with the simulations are provided in Table 2.

Table 2
Apparent first-order rate constants for Fe^{IV}-oxo formation and decay in wild-type TauD and selected variants using 21% or 100% O_2

TauD species	Final $[O_2]$			
	0.121 mM		0.575 mM	
	k_1 (s^{-1})	k_2 (s^{-1})	k_1 (s^{-1})	k_2 (s^{-1})
Wild-type	31 ± 3	12 ± 3	80 ± 5	13 ± 2
D101E	4.5 ± 3	2 ± 2	7 ± 3	3 ± 3
H255E	30 ± 2	12 ± 1	70 ± 7	15 ± 3
H255Q	25 ± 2	11 ± 3	90 ± 8	12 ± 2

ligand-to-metal charge-transfer (LMCT) transitions in TauD [23,31]. Those LMCT spectra form upon mixing αKG–Fe^{II}–TauD or succinate-Fe^{II}–TauD with buffer saturated with 100% oxygen, resulting in the oxidative modification of Tyr73 by two distinct mechanisms [32] to form

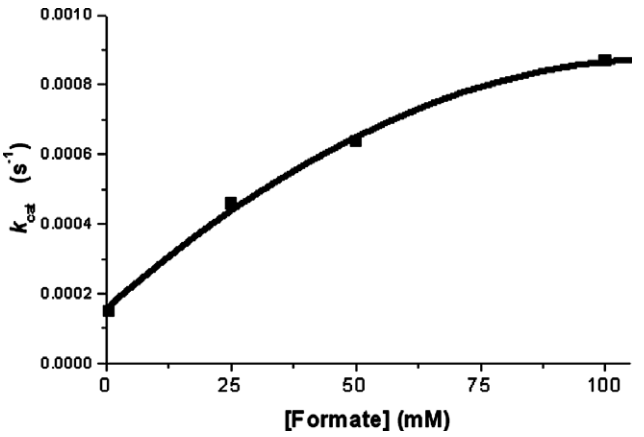

Fig. 3. Activation of D101A TauD by formate. The k_{cat} of the D101A variant was determined in standard assay buffer containing the indicated concentrations of formate.

dihydroxyphenylalanine (DOPA) that chelates the oxidized metal (steps A and B in Scheme 3). When this aberrant reaction is driven by αKG decomposition, it results in a chromophore (λ_{max} 550 nm, $\varepsilon_{550} = 460$–$700\ M^{-1}\,cm^{-1}$) distinct from that formed in the presence of succinate (λ_{max} 720 nm, ε_{720} $380\ M^{-1}\,cm^{-1}$); protein samples exhibiting these features have the same catecholate–Fe^{III} metallocenter, but with bicarbonate bound to the metal in the first case and not the second. Evidence supporting this assignment includes the ability to experimentally interconvert the two species [31]. In the present study, DOPA interaction with Fe^{II} under *anaerobic* conditions cannot account for the observed spectra since there is no means to oxidize the metal; however, the spectra of interest could arise from DOPA quinone (generated spontaneously by oxidation of DOPA; step C of Scheme 3) reacting with excess Fe^{II} (to supply additional reductant) to form a catecholate–Fe^{III} LMCT (Scheme 3, step D).

Several experiments were carried out to test the hypothesis that small amounts of Tyr73-derived DOPA quinone are present in wild-type TauD and the D101E, H255Q, and H255E variants as isolated from aerobically grown cells. First, when Fe^{II} was added to TauD purified from anaerobically grown cells, no 650 nm chromophore was generated (data not shown) consistent with the lack of DOPA quinone formation in the absence of oxygen. Second, the TauD isolated from aerobically grown cells was treated with 4 equivalents of $NaBH_4$ to reduce to DOPA any DOPA quinone that might be present. The addition of Fe^{II} to this sample failed to generate the 650 nm species, but the sample was capable of generating the standard Fe/αKG and Fe/αKG/taurine spectra (Fig. 4b). Third, active TauD variants with Tyr73 replaced by Ile or Ser [23] were shown to be incapable of chromophore formation when Fe^{II} was added to anaerobic samples (data not shown). Finally, a quinone-staining procedure was used to demonstrate the presence of such a redox-active species in each of the proteins capable of forming the 650 nm chromophore, but not for other mutant protein samples or for TauD

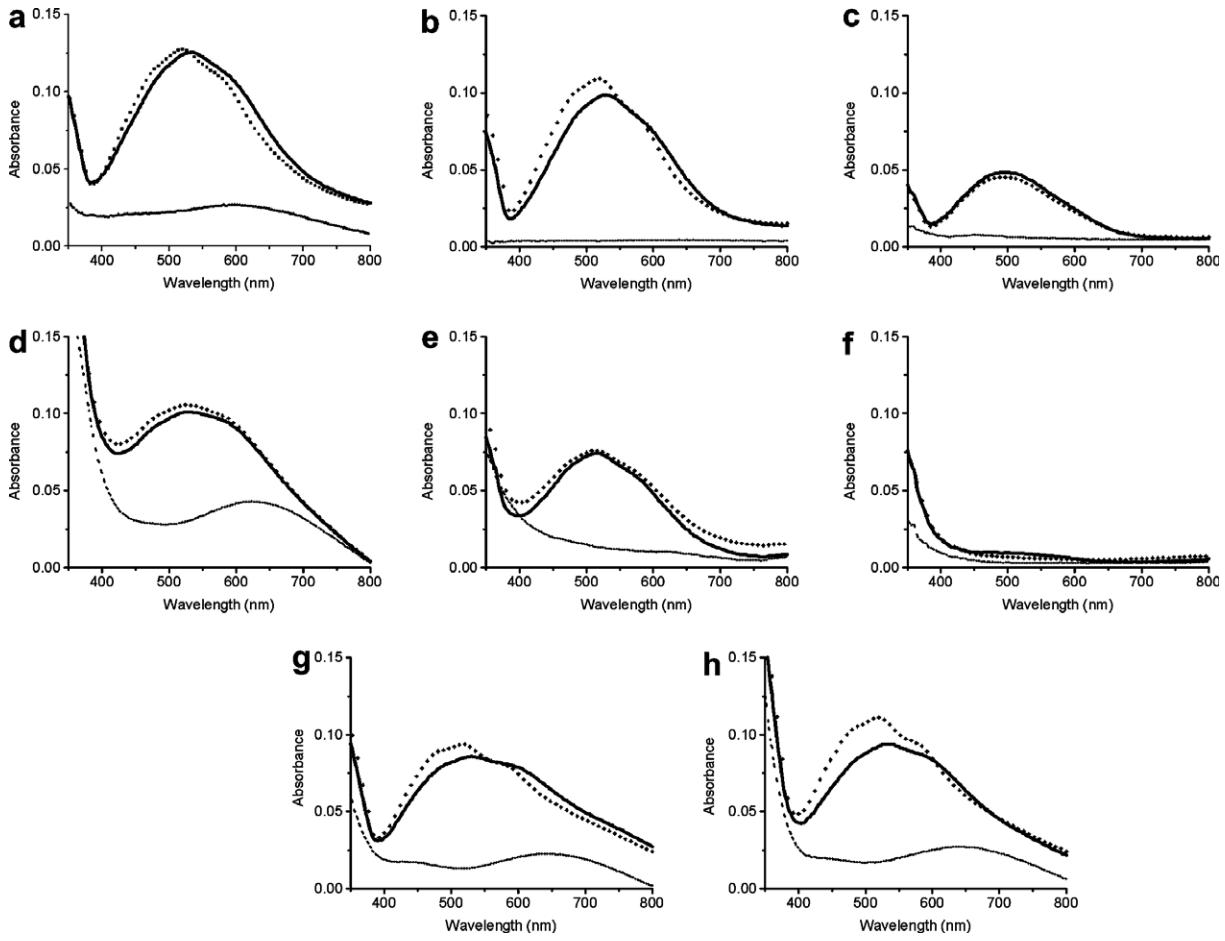

Fig. 4. Effects of ligand substitutions on TauD chromophores generated by sequential addition of Fe^{II}, αKG, and taurine. TauD samples (500 μM subunit concentration except where indicated) in 25 mM Tris, pH 8.0, buffer were made anaerobic in a sealed cuvette and scanned, a mixture of Fe^{II} and ascorbate was added (final concentrations of 500 μM and 100 μM, respectively), and scans were recorded before and after adjusting to 2 mM αKG and then 2 mM taurine. Difference spectra (with the spectrum of TauD apoprotein subtracted) are depicted for the Fe^{II}–TauD, αKG–Fe^{II}–TauD, and taurine–αKG–Fe^{II}–TauD species (dashed, solid, and dotted lines, respectively) of (a) wild-type enzyme, (b) wild-type enzyme that had been treated with four equivalents of $NaBH_4$, and the following TauD variants: (c) H99A, (d) D101E, (e) D101Q, (f) D101A (230 μM), (g) H255E, and (h) H255Q. Spectra of additional variants are available in Fig. S1.

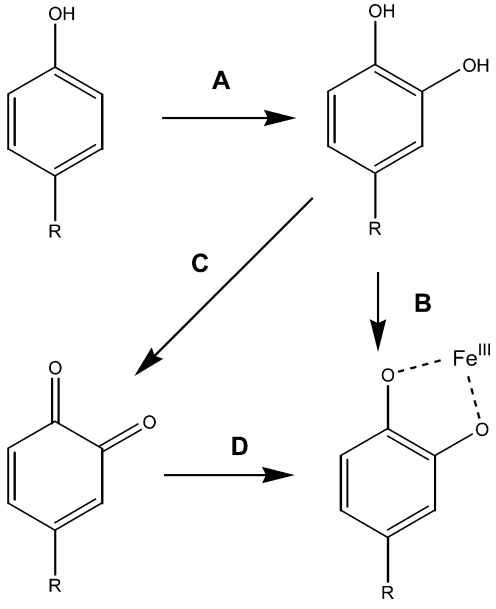

Scheme 3.

obtained from anaerobically grown cultures (a selection of samples is depicted in Fig. 5). We conclude that wild-type TauD and the three highly active mutants use intracellular Fe^{II}, αKG, succinate, and O_2 to create a DOPA side chain by using established reactions, and that a portion of this modified residue is oxidized to the quinone state either in the aerobic culture or as the protein is purified aerobically. In contrast, inactive variants are unable to activate oxygen to achieve side chain hydroxylation and cannot form the quinone. While the presence of DOPA had been described previously in TauD [23,31,32], its oxidation to the quinone state and chromophore generation upon addition of Fe^{II} to anaerobic enzyme samples are new findings.

3.5. Effects of metal ligand substitutions on the αKG–Fe^{II}–TauD and taurine–αKG–Fe^{II}–TauD spectra

TauD variants with altered metal-binding residues were examined for their abilities to properly fold and bind Fe^{II}, αKG, and taurine by comparing their electronic spectra to

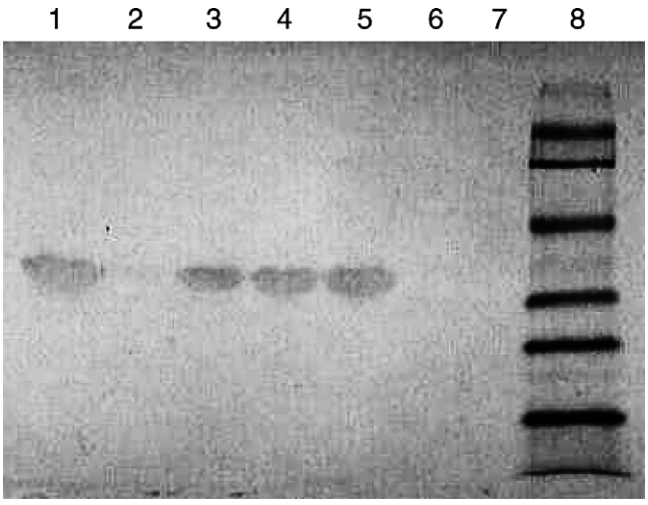

Fig. 5. Quinone stain analysis of TauD samples. Proteins were treated by SDS–PAGE, transferred to nitrocellulose, and analyzed by using the NBT staining procedure for detection of quinoproteins. Lanes: 1, wild-type TauD isolated from aerobically grown cultures; 2, wild-type TauD purified from anaerobically grown cells; 3, D101E; 4, H255E; 5, H255Q; 6, H99Q; 7, D101Q variants of TauD; and 8, pre-stained low-range molecular markers (Bio-Rad).

those of wild-type enzyme (Figs. 4 and S1). The latter protein forms a lilac-colored species (λ_{max} 530 nm, ε_{530} 250 M^{-1} cm^{-1}) in the presence of Fe^{II} and αKG (Fig. 4a, solid line), and this species shifts to higher energy and becomes more featured (dotted line) in the presence of taurine (λ_{max} 520 nm, ε_{520} 254 M^{-1} cm^{-1}). These spectra are associated with MLCT transitions that arise from Fe^{II} chelation by αKG [13–15] and are associated with the six-coordinate and five-coordinate metal species corresponding to species B and C in Scheme 2.

None of the His99 variants develop the MLCT features of wild-type enzyme, but several of the αKG-bound species absorb weakly at about 500 nm ($\varepsilon_{500} \sim 25$ M^{-1} cm^{-1}) as illustrated by the spectrum of the H99A sample (Fig. 4c). Subsequent addition of taurine has no significant effect on the spectra of these mutant proteins. The inability to generate the 530 and 520 nm spectra correlates well with the low activity of these variants.

Several of the Asp101 variants exhibit spectra resembling the wild-type enzyme in the presence of Fe^{II} and αKG. In particular, the αKG–Fe^{II}–D101E sample (Fig. 4d) exhibits a near wild-type MLCT, but at about 2/3 of the intensity of native enzyme ($\varepsilon_{520} = 152$ M^{-1} cm^{-1}). Progressively less intense spectra at increasingly higher energies are associated with the Fe^{II}- and αKG-bound form of the less active D101Q ($\varepsilon_{515} = 125$ M^{-1} cm^{-1}, Fig. 4e), D101N ($\varepsilon_{505} = 104$ M^{-1} cm^{-1}), and D101C ($\varepsilon_{495} = 72$ M^{-1} cm^{-1}) proteins (the latter two spectra are provided in Fig. S1). In contrast, the D101A sample (Fig. 4f) shows no convincing Fe^{II}/αKG-associated chromophore; this is the case even in the presence of 100 mM formate (data not shown) suggesting that the additive does not confer the normal metallocenter properties to a significant fraction of this protein. Subsequent addition of taurine to several of the Asp101 variant samples results in little change to the spectra, compatible with a less clear shift from six- to five-coordinate geometry. Because these Fe^{II}- and αKG-bound variant samples exhibit spectra that are shifted to higher energy compared to the native enzyme, it is possible that they already possess five-coordinate metallocenters.

The spectra of two His255 variants most closely resemble the spectra of wild-type enzyme. Specifically, the αKG- and Fe^{II}-bound forms of H255E (Fig. 4g) and H255Q (Fig. 4h) TauD exhibit λ_{max} of 530 nm with ε_{530} of 151 and 144 M^{-1} cm^{-1}, respectively. Furthermore, the addition of taurine to these proteins perturbs their spectra to yield maxima at higher energies and greater intensities (λ_{max} of 520 nm with ε_{520} of 187 and 153 M^{-1} cm^{-1}, respectively), as seen with wild-type enzyme. In contrast to these two mutant proteins, no significant chromophores are observed in the other His255 variants (Fig. S1).

3.6. Effects of metal ligand substitutions on the Co^{II}–TauD, αKG–Co^{II}–TauD, taurine–αKG–Co^{II}–TauD spectra

As an independent approach to examine the metallocenter properties of the TauD variants, Co^{II}-substituted proteins were studied. As described earlier [28] and illustrated in Fig. 6a, the addition of Co^{II} to an anaerobic sample of TauD yields a broad feature at ~520 nm ($\varepsilon_{520} \sim 50$ M^{-1} cm^{-1}) that is unchanged by αKG amendment. Subsequent inclusion of taurine leads to a distinct spectrum with significant transitions at 500, 552, and (of greatest intensity) 565 nm ($\varepsilon_{565} = 204$ M^{-1} cm^{-1}). The magnitude of the Co^{II} extinction coefficient empirically correlates to its coordination number in proteins [33], with six-coordinate sites having extinction coefficients about 50 M^{-1} cm^{-1}, five-coordinate sites with values of 50–300 M^{-1} cm^{-1}, and four-coordinate sites possessing coefficients of more than 300 M^{-1} cm^{-1}. These results suggest that the Co^{II} sites in Co^{II}–TauD and αKG–Co^{II}–TauD are six-coordinate, whereas that in taurine–αKG–Co^{II}–TauD is five-coordinate. Thus, the binding of substrate leads to the dissociation of a water molecule in this metal-substituted protein just as in the active Fe^{II}-containing enzyme. Analogous results were found when using the alternate substrates MOPS and PSA (data not shown), but with less pronounced absorption features for the αKG- and sulfonate-bound species ($\varepsilon_{565} = 127$ M^{-1} cm^{-1} and 133 M^{-1} cm^{-1}, respectively) than what was observed for taurine. We attribute the less intense chromophores to the larger K_d values of these compounds than for taurine, compatible with the reported K_m values of the Fe^{II}-containing enzyme (0.44 mM, 2.6 mM, and 58 μM, respectively, for MOPS, PSA, and taurine) [12]. We examined the spectra of Co^{II}-substituted variant proteins to determine whether they are able to bind metal and substrates in a productive configuration.

The spectra of selected Co^{II}-substituted TauD variants are illustrated in Fig. 6 (with other spectra available as Fig. S2). The H99A variant protein (Fig. 6b) exhibits an

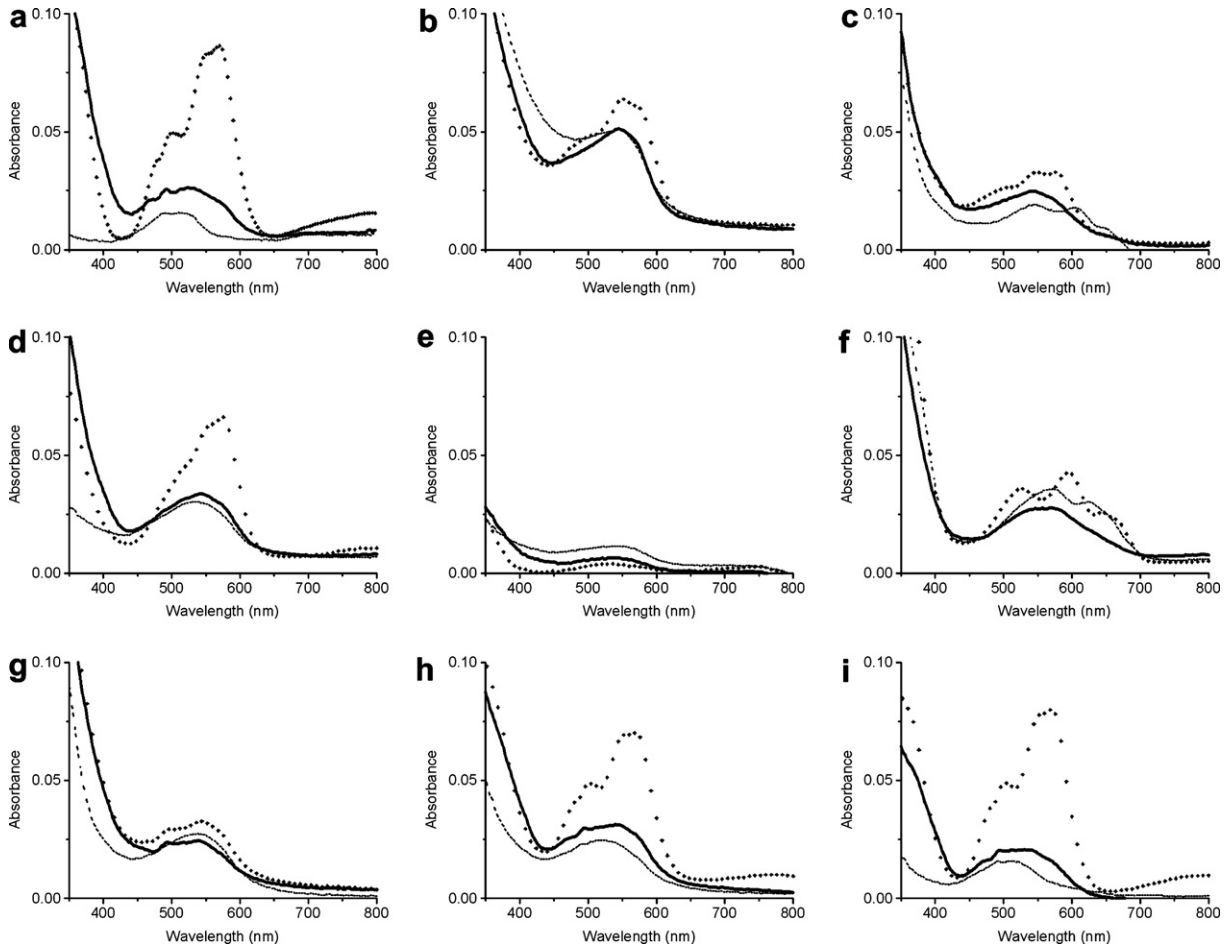

Fig. 6. Effects of ligand substitutions on TauD chromophores generated by sequential addition of Co^{II}, αKG, and taurine. TauD samples (500 μM subunit) in 25 mM Tris, pH 8.0, buffer were scanned and the samples were sequentially adjusted to contain 500 μM Co^{II}, 2 mM αKG, and 2 mM taurine. Difference spectra (with the apoprotein spectrum subtracted) are shown for the Co^{II}–TauD (dashed lines), KG–Co^{II}–TauD (solid lines), and taurine–αKG–Co^{II}–TauD (dotted lines) species for (a) wild-type TauD and the following TauD variants: (b) H99A, (c) H99C, (d) H99E, (e) D101A, (f) D101C, (g) D101E, (h) H255E, and (i) H255Q. Additional spectra are provided in Fig. S2.

increase in absorbance at ~550 nm upon binding both αKG and taurine, but the final intensity ($\varepsilon_{550} = 120\ M^{-1}\ cm^{-1}$) is much smaller and at higher energy than for the wild-type enzyme. The spectrum of taurine–αKG–Co^{II}–H99E protein (Fig. 6d) is similar to, but less intense ($\varepsilon_{550} = 132\ M^{-1}\ cm^{-1}$), than that of the wild-type protein. The spectrum of the Co^{II}-bound H99C variant (Fig. 6c) reveals discrete transitions at longer wavelengths (610 and 650 nm) that are not observed in the wild-type protein; we attribute these features to ligand field effects associated with thiolate coordination to the metal ion, but the data do not prove that this residue is a ligand. The addition of αKG to this sample produces a more typical appearance of the spectrum, and subsequent addition of taurine leads to a small increase in intensity at 590 nm – again at lower energy than for wild-type protein. The spectra of the H99Q and H99N variants (Supplementary data) show slight changes after addition of substrates, but do not appear to undergo a clear change of coordination number. Finally, the H99D sample tends to precipitate in the presence of Co^{II}, so no useful information is available from these spectra.

Two Asp101 variants exhibit clear evidence for binding Co^{II} at their catalytic sites, whereas most of the mutant proteins yield only the d–d transitions associated with the six-coordinate metal ion (e.g., as seen in the D101A variant in Fig. 6e). Supplementation of the latter sample with 100 mM formate did not restore the wild-type spectrum, indicating that the chemical rescue suggested by the slight activity increase was very incomplete. The spectrum of Co^{II}–D101C TauD (Fig. 6f) somewhat resembles that of the H99C variant by revealing discrete long wavelength transitions (565 and 630 nm) distinct from the spectrum of Co^{II}–TauD. As in the H99C case, the addition of αKG to the Co^{II}–D101C protein leads to a more typical appearance of the spectrum, with a λ_{max} at 575 nm. Subsequent addition of taurine to the D101C sample generates a unique spectrum containing transitions at 525, 585, and 650 nm, likely due to ligand field effects from the metal-bound thiolate. Precedent for added ligands perturbing the spectra of Co^{II}-substituted proteins to yield similar features toward longer wavelength are reported for aminopeptidase and angiotensin converting enzyme [34,35]. The

αKG–Co^{II}–D101E TauD spectrum (Fig. 6g) increases in intensity upon binding taurine, as seen for wild-type protein, but the effect is much smaller. We attribute this result to only a partial conversion of six-coordinate to five-coordinate geometry for the metal ion in this variant protein.

The spectra of two Co^{II}-substituted His255 variants, H255E and H255Q (Fig. 6h and i), closely resemble those of the wild-type enzyme. Thus, both proteins exhibit large enhancements in absorbance at 565 nm upon binding taurine (ε_{565} of 136 and 177 M^{-1} cm^{-1}, respectively) consistent with substrate-promoted loss of water and formation of a five-coordinate site. In contrast to these variants, the spectra of other Co^{II}-substituted His255 variants of TauD (Fig. S2) are essentially unchanged by addition of αKG or taurine.

3.7. Relationship of the TauD results to mutagenesis studies of other family members

The His99 residue of TauD, coplanar with the bound αKG, is critical for generating a highly active form of the enzyme. Trace activity was detected in several variants at this position, but the corresponding kinetic parameters could not be reliably estimated. Similar to our results using TauD, variants affecting the comparable ligand position for other Fe^{II}/αKG-dependent dioxygenases all are inactive except for the 0.15% active Gln derivative of flavanone 3β-hydroxylase [36] (Table S1). For example, various substitutions of the His ligands in the protein-modifying enzymes collagen-specific prolyl 4-hydroxylase [37], hypoxia-inducible factor (HIF)-specific prolyl 4-hydroxylase [38], lysyl hydroxylase [39], and histone demethylase [40] are inactive. Similar results are reported for metabolite-transforming enzymes such as phytanoyl-CoA hydroxylase (PAHX) [41,42], CAS [43], 2,4-dichlorophenoxyacetic acid hydroxylase (TfdA) [44], and a bacterial ethylene-forming enzyme [45]. For the sequence-related αKG-independent enzymes 1-aminocyclopropane-1-carboxylate (ACC) oxidase and isopenicillin *N* synthase (IPNS), the comparable His residue in each protein was extensively mutagenized and all of the variants are inactive except for 1% of the wild-type activity reported for H177Q ACC oxidase [46–52]. In marked contrast, substitution of the His ligand by Ala in (*S*)-2-hydroxypropylphosphonic acid epoxidase (HppE) led to an enzyme variant that retains 20% of the activity of the wild-type enzyme [53]. HppE is another αKG-independent dioxygenase related in sequence to TauD, but it possesses a His-Xxx-Yyy-Glu-$(Xxx)_n$-His metal-binding ligand motif [54] rather than the His-Xxx-Asp/Glu-$(Xxx)_n$-His motif uniformly found in Fe^{II}/αKG-dependent dioxygenases [1]. The extra spacing between the His and carboxylate in HppE is consistent with greater flexibility in this region of the protein, perhaps allowing another residue to substitute for His in the H138A HppE variant. Within the Fe^{II}/αKG-dependent hydroxylase enzyme family, a His residue at this position appears to be crucial for high levels of activity.

The Asp101 residue of TauD can only be substituted effectively by the alternative carboxylate Glu as judged by retention of enzyme activity or capacity to form the Fe^{II} and Co^{II} metallocenter chromophores. Trace levels of activity are detected in several other variants at this position. Substitution of the corresponding Asp residue in other family representatives (Table S1) also leads to significant activity loss, unless the substitution is by Glu. In particular, nearly complete activity losses were reported when various residues are substituted for the corresponding Asp in HIF-specific prolyl hydroxylase [38], lysyl hydroxylase [39], PAHX [41,42], flavanone β-hydroxylase [36], TfdA [44], and some mutant versions of collagen-specific prolyl 4-hydroxylase [55]. Of interest, however, substitution of Asp by Glu in the latter enzyme still affords 15% of wild-type activity [55]. In the αKG-independent enzymes ACC oxidase and IPNS, replacement of the Asp ligands by other residues greatly affects activity; however, the D179E version of ACC oxidase and the D216E form of IPNS each retain 1% of the wild-type activity. Significantly, a Glu residue naturally occupies this position in CAS [56], histone demethylase [57], an uncharacterized family member from *Arabidopsis thalia* [58], and the non-αKG-dependent enzyme HppE [54]. The Ala variant of HppE is inactive. In this wild-type protein, the carboxylate is separated from the first His ligand by two residues and this spacing might require the longer side chain form of a carboxylate. Finally, the corresponding position in the syringomycin biosynthesis component SyrB2 is an Ala, and the metal ligand is replaced by chloride ion in this αKG-dependent halogenating enzyme [59]. Wondering whether D101A TauD might exhibit halogenating capability, we sought evidence for uncoupled αKG consumption in buffer containing taurine and varied chloride concentrations; however, we were unable to obtain any evidence for the presence of chlorinating activity in this variant. In general, an Asp or Glu residue must occupy this position within the Fe^{II}/αKG-dependent hydroxylases.

His255 of TauD, located opposite the site of oxygen binding, can be substituted by Gln or Glu to produce highly active proteins capable of generating the typical metal-dependent chromophores. Furthermore, trace levels of activity are found when Asn or Ala replace this metal-binding ligand. These results are generally compatible with mutagenesis studies of other family members (Table S1), but some differences are noted. All three variants at this position of collagen prolyl 4-hydroxylase are inactive, including that substituted with Glu [37]. Several variants of aspartyl(asparaginyl) hydroxylase are inactive, including that substituted with Gln, whereas the Asp and Glu forms are 20% and 12% active [60]; however, it should be noted that no firm evidence exists to identify this ligand in the enzyme. While substitution by Ala eliminates activity in two HIF-specific prolyl 4-hydroxylases [38,61] and TfdA [44], the Ala variant retains 7.5% of the wild-type activity in PAHX [42] and fully 35% of the activity in HABH3 [62]. Gln-substituted CAS and flavanone 3β-

hydroxylase are inactive [36,43], yet this form of ethylene-forming enzyme retains slight activity [45]. All variants of the corresponding His residue in the αKG-independent family members are inactive, even the Gln and Glu versions of ACC oxidase [48] and the Glu variant of IPNS [52]. Thus, it appears that the activity of variant proteins substituted at this position is dependent on the particular protein.

4. Conclusion

The results described above present the first extensive analysis of the effects of varying the metal-binding residues for any Fe^{II}/αKG-dependent hydroxylase. The ligands that are coplanar with the αKG are unalterable (His99) or can only be substituted by Glu (Asp101), whereas the ligand positioned opposite of the O_2 binding site (His255) can be replaced by Gln or Glu while retaining high levels of activity. For all of the highly active variants the ability to form diagnostic Fe^{II}- or Co^{II}-dependent chromophores is retained. In addition, we obtained evidence for partial activation of the D101A variant by formate. Structural or spectroscopic studies will be needed to confirm that the proposed additive functionally replaces (i.e., chemically rescues) the side chain ligand. Finally, we provided evidence for the presence of DOPA quinone in the wild-type enzyme and highly active variants that are capable of activating oxygen. The quinone is likely to form by spontaneous oxidation of DOPA that is generated during aerobic growth of cells producing TauD.

5. Abbreviations

αKG	alpha-ketoglutarate
ACC	1-aminocyclopropane-1-carboxylate
AlkB	methylated DNA (1-methyladenine/3-methylcytosine) repair enzyme
CAS	clavaminate synthase
DOPA	dihydroxyphenylalanine
HABH3	human AlkB homologue isozyme 3
HIF	hypoxia-inducible factor
HppE	(*S*)-2-hydroxypropylphosphonic acid epoxidase
IPNS	isopenicillin *N* synthase
LMCT	ligand-to-metal charge-transfer
MLCT	metal-to-ligand charge-transfer
MOPS	3-*N*-morpholinopropanesulfonic acid
NBT	nitroblue tetrazolium
PAHX	phytanoyl-CoA hydroxylase
PSA	pentanesulfonic acid
SDS–PAGE	sodium dodecyl sulfate–polyacrylamide gel electrophoresis
TauD	taurine/αKG dioxygenase
TfdA	2,4-dichlorophenoxyacetic acid/αKG dioxygenase
UV	ultraviolet

Acknowledgments

We thank David Ballou for use of his stopped-flow instrument, Tatyana Spolitak for assistance in setting up that equipment, Greta Monterosso for creating some of the variants, Scott Mulrooney and other members of the Hausinger laboratory for their kind assistance, and a reviewer for useful suggestions. These studies were supported by the National Institutes of Health Grant GM063584.

Appendix A. Supplementary data

Table S1 summarizes metal ligand identification and mutagenesis studies in other family members, and Figs. S1 and S2 show additional spectra of Fe^{II} and Co^{II} forms of variant TauD species, respectively. Supplementary data associated with this article can be found, in the online version, at doi:10.1016/j.jinorgbio.2007.01.011.

References

[1] R.P. Hausinger, Crit. Rev. Biochem. Mol. Biol. 39 (2004) 21–68.
[2] F.H. Vaillancourt, E. Yeh, D.A. Vosburg, S.E. O'Conner, C.T. Walsh, Nature 436 (2005) 1191–1194.
[3] F.H. Vaillancourt, J. Yin, C.T. Walsh, Proc. Natl. Acad. Sci. USA 102 (2005) 10111–10116.
[4] E. Eichhorn, J.R. van der Ploeg, M.A. Kertesz, T. Leisinger, J. Biol. Chem. 272 (1997) 23031–23036.
[5] H.M. Hanauske-Abel, V. Günzler, J. Theor. Biol. 94 (1982) 421–455.
[6] E.L. Hegg, L. Que Jr., Eur. J. Biochem. 250 (1997) 625–629.
[7] K.D. Koehntop, J.P. Emerson, L. Que Jr., J. Biol. Inorg. Chem. 10 (2005) 87–93.
[8] I.J. Clifton, M.A. McDonough, D. Ehrismann, N.J. Kershaw, N. Granatino, C.J. Schofield, J. Inorg. Biochem. 100 (2006) 644–669.
[9] J.M. Elkins, M.J. Ryle, I.J. Clifton, J.C. Dunning Hotopp, J.S. Lloyd, N.I. Burzlaff, J.E. Baldwin, R.P. Hausinger, P.L. Roach, Biochemistry 41 (2002) 5185–5192.
[10] J.R. O'Brien, D.J. Schuller, V.S. Yang, B.D. Dillard, W.N. Lanzilotta, Biochemistry 42 (2003) 5547–5554.
[11] M.J. Ryle, R. Padmakumar, R.P. Hausinger, Biochemistry 38 (1999) 15278–15286.
[12] P.K. Grzyska, M.J. Ryle, G.R. Monterosso, J. Liu, D.P. Ballou, R.P. Hausinger, Biochemistry 44 (2005) 3845–3855.
[13] E.G. Pavel, J. Zhou, R.W. Busby, M. Gunsior, C.A. Townsend, E.I. Solomon, J. Am. Chem. Soc. 120 (1998) 743–753.
[14] J. Zhou, M. Gunsior, B.O. Bachmann, C.A. Townsend, E.I. Solomon, J. Am. Chem. Soc. 120 (1998) 13539–13540.
[15] J. Zhou, W.L. Kelly, B.O. Bachmann, M. Gunsior, C.A. Townsend, E.I. Solomon, J. Am. Chem. Soc. 123 (2001) 7388–7398.
[16] R.Y.N. Ho, M.P. Mehn, E.L. Hegg, A. Liu, M.A. Ryle, R.P. Hausinger, L. Que Jr., J. Am. Chem. Soc. 123 (2001) 5022–5029.
[17] J.C. Price, E.W. Barr, B. Tirupati, J.M. Bollinger Jr., C. Krebs, Biochemistry 42 (2003) 7497–7508.
[18] J.C. Price, E.W. Barr, T.E. Glass, C. Krebs, J.M. Bollinger Jr., J. Am. Chem. Soc. 125 (2003) 13008–13009.
[19] J.C. Price, E.W. Barr, L.M. Hoffart, C. Krebs, J.M. Bollinger Jr., Biochemistry 44 (2005) 8138–8147.
[20] P.J. Riggs-Gelasco, J.C. Price, R.B. Guyer, J.H. Brehm, E.W. Barr, J.M. Bollinger Jr., C. Krebs, J. Am. Chem. Soc. 126 (2004) 8108–8109.
[21] D.A. Proshlyakov, T.F. Henshaw, G.R. Monterosso, M.J. Ryle, R.P. Hausinger, J. Am. Chem. Soc. 126 (2004) 1022–1023.
[22] L.M. Hoffart, E.W. Barr, R.B. Guyer, J.M. Bollinger Jr., C. Krebs, Proc. Natl. Acad. Sci. USA 103 (2006) 14738–14743.

[23] M.J. Ryle, A. Liu, R.B. Muthukumaran, R.Y.N. Ho, K.D. Koehntop, J. McCracken, L. Que Jr., R.P. Hausinger, Biochemistry 42 (2003) 1854–1862.
[24] U.K. Laemmli, Nature (London) 227 (1970) 680–685.
[25] M.M. Bradford, Anal. Biochem. 72 (1976) 248–254.
[26] B. Miroux, J.E. Walker, J. Mol. Biol. 260 (1996) 289–298.
[27] H. Beinert, Meth. Enzymol. 54 (1978) 435–445.
[28] E. Kalliri, P.K. Grzyska, R.P. Hausinger, Biochem. Biophys. Res. Commun. 338 (2005) 191–197.
[29] P.R. Bevington, in: Data Reduction and Error Analysis for the Physical Sciences, McGraw-Hill, New York, 1969, pp. 235–242.
[30] M.A. Paz, R. Flückiger, A. Boak, H.M. Kagan, P.M. Gallop, J. Biol. Chem. 266 (1991) 689–692.
[31] M.J. Ryle, K.D. Koehntop, A. Liu, L. Que Jr., R.P. Hausinger, Proc. Natl. Acad. Sci. USA 100 (2003) 3790–3795.
[32] K.D. Koehntop, S. Marimanikkuppam, M.J. Ryle, R.P. Hausinger, L. Que Jr., J. Biol. Inorg. Chem. 11 (2006) 63–72.
[33] I. Bertini, C. Luchinat, in: G.L. Eichhorn, L.G. Marzilli (Eds.), Advances in Inorganic Biochemistry, Elsevier, Amsterdam, 1984, pp. 71–111.
[34] R. Bicknell, B. Holmquist, F.S. Lee, M.T. Martin, J.F. Riordan, Biochemistry 26 (1987) 7291–7297.
[35] D.L. Bienvenue, B. Bennett, R.C. Holz, J. Inorg. Biochem. 78 (2000) 43–54.
[36] R. Lukacin, L. Britsch, Eur. J. Biochem. 249 (1997) 748–757.
[37] J. Myllyharju, K.I. Kivirikko, EMBO J. 16 (1997) 1173–1180.
[38] R.K. Bruick, S.L. McKnight, Science 294 (2001) 1337–1340.
[39] A. Pirskanen, A.-M. Kaimio, R. Myllylä, K.I. Kivirikko, J. Biol. Chem. 271 (1996) 9398–9402.
[40] P.A.C. Cloos, J. Christensen, K. Agger, A. Maiolica, J. Rappsilber, T. Antal, K.H. Hansen, K. Helin, Nature 442 (2006) 307–311.
[41] T. Searls, D. Butler, W. Chien, M. Mukherji, M.D. Lloyd, C.J. Schofield, J. Lipid Res. 46 (2005) 1660–1670.
[42] M. Mukherji, W. Chien, N.J. Kershaw, I.J. Clifton, C.J. Schofield, A.S. Wierzbicki, M.D. Lloyd, Hum. Mol. Genet. 10 (2001) 1971–1982.
[43] N. Khaleeli, R.W. Busby, C.A. Townsend, Biochemistry 39 (2000) 8666–8673.
[44] D.A. Hogan, S.R. Smith, E.A. Saari, J. McCracken, R.P. Hausinger, J. Biol. Chem. 275 (2000) 12400–12409.
[45] K. Nagahama, K. Yoshini, M. Matsuoka, S. Tanase, T. Ogawa, H. Fukuda, J. Ferm. Bioeng. 85 (1998) 255–258.
[46] J.-F. Shaw, Y.-S. Chou, R.-C. Chang, S.F. Yang, Biochem. Biophys. Res. Commun. 225 (1996) 697–700.
[47] V.J. Lay, A.G. Prescott, P.G. Thomas, P. John, Eur. J. Biochem. 242 (1996) 228–234.
[48] Z. Zhang, J.N. Barlow, J.E. Baldwin, C.J. Schofield, Biochemistry 36 (1997) 15999–16007.
[49] I. Borovok, O. Landman, R. Kreisberg-Zakarin, Y. Aharonowitz, G. Cohen, Biochemistry 35 (1996) 1981–1987.
[50] D.S.H. Tan, T.-S. Sim, J. Biol. Chem. 271 (1996) 889–894.
[51] P. Loke, J. Sim, T.-S. Sim, FEMS Microbiol. Lett. 157 (1997) 137–140.
[52] R. Kreisberg-Zakarin, I. Borovok, M. Yanko, F. Frolow, Y. Aharonowitz, G. Cohen, Biophys. Chem. 86 (2000) 109–118.
[53] F. Yan, T. Li, J.D. Lipscomb, A. Liu, H.-W. Liu, Arch. Biochem. Biophys. 442 (2005) 82–91.
[54] L.J. Higgins, F. Yan, P. Liu, H.-W. Liu, C.L. Drennan, Nature 437 (2005) 838–844.
[55] A. Lamberg, T. Pihlajaniemi, K.I. Kivirikko, J. Biol. Chem. 270 (1995) 9926–9931.
[56] Z. Zhang, J. Ren, D.K. Stammers, J.E. Baldwin, K. Harlos, C.J. Schofield, Nat. Struct. Biol. 7 (2000) 127–133.
[57] Z. Chen, J. Zang, J.R. Whetstine, X. Hong, F. Davrazou, T.G. Kutateladze, M. Simpson, Q. Mao, C.-H. Pan, S. Dai, J. Hagman, K. Hansen, Y. Shi, G. Zhang, Cell 125 (2006) 691–702.
[58] E. Bitto, C.A. Bingman, S.T. Allard, G.E. Wesenberg, D.J. Aceti, R.L. Wrobel, R.O. Frederick, H. Sreenath, F.C. Vojtik, W.B. Jeon, C.S. Newman, J. Primm, M.R. Sussman, B.G. Fox, J.L. Markley, G.N. Phillips Jr., Acta Crystallogr., Sect. F 61 (2005) 469–472.
[59] L.C. Blasiak, F.H. Vaillancourt, C.T. Walsh, C.L. Drennan, Nature 440 (2006) 368–371.
[60] K. McGinnis, G.M. Ku, W.J. VanDusen, J. Fu, V. Garsky, A.M. Stern, P.A. Friedman, Biochemistry 35 (1996) 3957–3962.
[61] A.C.R. Epstein, J.M. Gleadle, L.A. McNeill, K.S. Hewitson, J. O'Rourke, D.R. Mole, M. Mukherji, E. Metzen, M.I. Wilson, A. Dhanda, Y.-M. Tian, N. Masson, D.L. Hamilton, P. Jaakkola, R. Barstead, J. Hodgkin, P.H. Maxwell, C.W. Pugh, C.J. Schofield, P.J. Ratcliffe, Cell 107 (2001) 43–54.
[62] O. Sundheim, C.B. Vågbo, M. Bjorås, M.M.L. Sousa, V. Talstad, P.A. Aas, F. Drablos, H.E. Krokan, J.A. Tainer, G. Slupphaug, EMBO J. 25 (2006) 3389–3397.